Structural Changes of Creatine Kinase upon Substrate Binding

Michael Forstner,* Manfred Kriechbaum,# Peter Laggner,# and Theo Wallimann*
*Institute of Cell Biology, Swiss Federal Institute of Technology Zürich, CH-8093 Zürich, Switzerland, and #Institute of Biophysics and X-Ray Structure Research, Austrian Academy of Sciences, A-8010 Graz, Austria

ABSTRACT Small-angle x-ray scattering was used to investigate structural changes upon binding of individual substrates or a transition state analog complex (TSAC; Mg-ADP, creatine, and KNO_3) to creatine kinase (CK) isoenzymes (dimeric muscle-type (M)-CK and octameric mitochondrial (Mi)-CK) and monomeric arginine kinase (AK). Considerable changes in the shape and the size of the molecules occurred upon binding of Mg-nucleotide or TSAC. The radius of gyration of Mi-CK was reduced from 55.6 Å (free enzyme) to 48.9 Å (enzyme plus Mg-ATP) and to 48.2 Å (enzyme plus TSAC). M-CK showed similar changes from 28.0 Å (free enzyme) to 25.6 Å (enzyme plus Mg-ATP) and to 25.5 Å (enzyme plus TSAC). Creatine alone did not lead to significant changes in the radii of gyration, nor did free ATP or ADP. AK also showed a change of the radius of gyration from 21.5 Å (free enzyme) to 19.7 Å (enzyme plus Mg-ATP), whereas with arginine alone only a minor change could be observed. The primary change in structure as seen with monomeric AK seems to be a Mg-nucleotide-induced domain movement relative to each other, whereas the effect of substrate may be of local order only. In CK, however, additional movements have to be involved.

INTRODUCTION

Creatine Kinase (CK, EC 2.7.2.3) is a key enzyme of cellular energy metabolism, catalyzing the reversible phosphoryl transfer from phosphocreatine to ADP (for a review see Wallimann et al., 1992). Substrates are bound specifically in a rapid equilibrium, random mechanism with product release being the rate-limiting step under physiological conditions. In addition to the productive reaction, CK also forms a dead-end inhibition or transition state analog complex with Mg-ADP, nitrate, and creatine (TSAC).

CK is present in vertebrate cells of high and fluctuating energy demand, e.g., muscle fibers, neurons, photoreceptors, spermatozoa, or electrocytes, where it regenerates ATP from phosphocreatine during cellular work. Several isoforms of the enzyme have been reported: cytosolic (M, muscle type; B, brain type) and mitochondrial isoenzymes. Three cytosolic isoenzymes exist in homo- or heterodimeric form (BB-, MB-, and MM-CK) and two mitochondrial CKs occur mainly as octamers (Mi_a- and Mi_b-CK) (Wyss et al., 1992). CK is a member of the family of guanidino kinases (ATP:guanidinophosphotransferases), enzymes with closely related primary sequences and large structural similarities (Mühlebach et al., 1994). Lobster arginine kinase (AK, EC 2.7.3.3) is another member of this family, being a monomeric protein of 40 kDa, whereas the cytosolic forms of CK can be regarded either as dimeric members of this protein family, having relative molecular masses of 86 kDa, or as octamers of 340 kDa, that can be dissociated into dimers in vitro, as found for Mi_b-CK (Gross and Wallimann, 1993).

Received for publication 18 February 1998 and in final form 12 May 1998.

Address reprint requests to Dr. Michael Forstner, Lawrence Livermore National Laboratory, Macromolecular Crystallography, LLNL-BBRP, L-452, Livermore, CA 94551. Tel.: 925-423-5427; Fax: 925-422-2282; E-mail: forstner1@llnl.gov.

0006-3495/98/08/1016/08 $2.00

Mi-CKs have been found in the intermembrane space of the mitochondria, being attached to the inner membrane (Rojo et al., 1991). The enzyme is thereby enabled to utilize intramitochondrially synthesized ATP for the synthesis of phosphocreatine, which is shuttled out of the mitochondria for the regeneration of ATP by the cytosolic CK isoenzymes. This interplay of mitochondrial and cytosolic CKs has been referred to as the phosphocreatine circuit (Wallimann et al., 1992).

Mi_b-CK from chicken heart has been crystallized in our laboratory (Schnyder et al., 1990), and its x-ray structure in the absence and presence of ATP (nota bene in the absence of Mg^{2+}) has been solved (Fritz-Wolf et al., 1996). The CK monomer displays a two-domain organization, with a small amino-terminal (residues 1–100) and a large carboxyl-terminal domain (residues 120–380). The latter is dominated by an eight-stranded antiparallel β-pleated sheet, surrounded by seven α-helices, whereas the amino-terminal domain exhibits helical structure elements only. Furthermore, a single β-strand formed by amino acids 121–130 separates the large β-sheet of the carboxyl-terminal domain in two halves, which, together with their surrounding structures, can be regarded as subdomains of the carboxy domain (C1 = 166–236, C2 = 287–316). Extensive monomer-monomer contacts allow for the formation of stable dimers from two Mi-CK monomers, whereas the dimers interact with each other only weakly, forming octameric assemblies. Fig. 1 shows the structural organization of a Mi_b-CK monomer. Two highly flexible loops (residues 60–65 and 314–321) in the structure that are characterized by crystallographic temperature factors above 40 $Å^2$ and were modeled by simulated annealing (Kirckpatrick et al., 1983; Brünger, 1991) to undergo movement toward the active site are indicated by arrows.

AK has been shown to undergo a decrease of the radius of gyration upon binding of Mg-ADP or Mg-ATP, which is

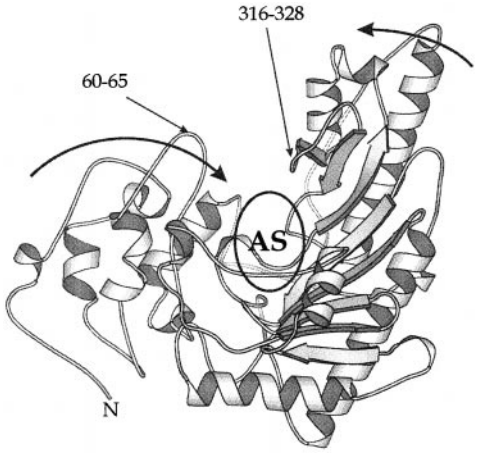

FIGURE 1 The creatine kinase monomer. The structural organization of an unligated Mi_b-CK monomer is shown. The location of the active site (AS) is roughly outlined by an ellipse. Two highly flexible loops (residues 60–65 and 316–328) in the structure that are characterized by crystallographic temperature factors above 40 $Å^2$ and were modeled by simulated annealing to undergo movement toward the active site are indicated by arrows. Bent arrows indicate the assumed primary movements of the domains relative to each other upon substrate binding. The figure was prepared from the x-ray coordinates of Mi_b-CK (Fritz-Wolf et al., 1996) using the program Molscript (Kraulis, 1991).

consistent with a hinge rotation of two domains (Dumas and Janin, 1983), and preliminary investigations suggested similar conformational changes for CK (Forstner et al., 1996). We now report the results from small-angle x-ray and neutron scattering (SAXS and SANS) experiments to investigate the structural behavior of mitochondrial octameric Mi_b-CK and cytosolic dimeric M-CK upon binding of their substrates. This approach offered a possibility to interpret data obtained by solution scattering based on the three-dimensional structure of the enzyme. We have also modeled the structure of M-CK from the coordinates of Mi_b-CK and compared the experimentally observed scattering curve with the one calculated from the model coordinates.

MATERIALS AND METHODS

Protein sources and sample preparation

Chicken sarcomeric mitochondrial creatine kinase (Mi_b-CK) was isolated from the *Escherichia coli* strain BL21(DE3)LysS transformed with the expression vector pRF23 and expressing the heterologous protein as described previously (Furter et al., 1992). Recombinant chicken muscle creatine kinase (M-CK) was isolated from *E. coli* transformed with an expression vector bearing the cDNA coding for this isoenzyme (M. Stolz, unpublished results). Lobster tail arginine kinase (AK) was obtained from commercial sources (Sigma Chemical Co., St. Louis, MO). All protein preparations were homogeneous as judged by Coomassie Blue-stained SDS-polyacrylamide gels. Enzyme activity was measured by the pH-stat method (Milner-White and Watts, 1971; Wallimann et al., 1984) in a buffer containing 75 mM KCl, 10 mM $MgCl_2$, 0.1 mM EGTA, and 1 mM β-mercaptoethanol. For routine checks of enzyme activity, phosphocreatine and ADP were added to a final concentration of 10 mM each, and the reaction was performed at pH 7.00. Protein concentrations were determined by the BioRad method (Bradford, 1976) using bovine serum albumin as a standard. Before use, proteins were dialyzed against a 100 mM sodium phosphate buffer (pH 7.4), containing 5 mM β-mercaptoethanol and 0.1 mM EDTA. For small-angle scattering measurements, final protein concentrations of 15, 10, 7.5, 5, and 2.5 mg/ml were used. The transition state analog complex (TSAC) consisted of 4 mM ADP, 5 mM $MgCl_2$, 20 mM creatine, and 50 mM KNO_3 (final concentrations). ATP was used at a final concentration of 20 mM with 40 mM $MgCl_2$ present.

Small-angle x-ray scattering experiments

SAXS measurements were carried out using a modified Kratky compact camera (MBraun-Graz-Optical Systems, Graz, Austria; Laggner and Mio, 1992), equipped with a linear position sensitive detector (MBraun, Garching, Germany) monitoring the scattering curves in the h range between 0.005 and 0.2 $Å^{-1}$ ($h = 4\pi \sin(\theta/\lambda)$, with 2θ being the scattering angle, and $\lambda = 1.5418$ Å being the wavelength of the x-rays). The line focus ($CuK_{\alpha a}$ radiation) of a RigakuRotoflex RU200 rotating anode generator (Rigaku Corp., Tokyo, Japan) was used, operating at 3 kW (50 kV and 60 mA). A 30-μm Ni filter was placed in front of the sample to eliminate the CuK_β radiation. The sample-detector distance was 272 mm, and the position calibration of the detector was performed using Ag-stearate as a reference material. The samples were measured in 1-mm (diameter) quartz capillaries, mounted in a steel cuvette, which provides good thermal contact to the Peltier heating unit. Measurements were performed at 4°C or 20°C, respectively, and exposure times were typically 1000 s for individual measurements. For data analysis, the results of three individual measurements were merged, background subtraction was performed, and the resulting data were deconvoluted with the slit width and slit length profiles of the primary beam and subsequently subjected to Fourier transformation using the program ITP (Glatter, 1977). Radii of gyration were further determined by the Guinier approximation from the low-h regions of the scattering curves employing the PS software (MBraun-Graz-Optical Systems) supplied with the SAXS detector, yielding also the intensity extrapolated to zero angle that was used in the subsequent calculation of relative molecular masses according to Luzatti (1960). To rule out radiation damage of the samples, protein was recovered from the cuvettes and enzymatic activity was determined.

Simulation of solution scattering curves

A computer program based on the algorithm of Lattman (1989) was used to calculate the x-ray scattering profile from the atomic coordinates of Mi-CK (Fritz-Wolf et al., 1996), based on the fact that the profile is the squared modulus of the rotationally averaged Fourier transform of the molecule. The program was written on an IBM-compatible PC using Borland C++ 4.5 (M. Forstner, unpublished). The scattering curve of M-CK was simulated from the coordinates of a molecular model dimer of M-CK, obtained as described below.

Molecular modeling

Homology modeling was performed using the software package SYBYL/COMPOSER (Tripos, St. Louis, MO) employing a combination of energy- and knowledge-based approaches. After sequence alignment of the sequences of chicken Mi_b-CK and M-CK, based on the Needleman-Wunsch algorithm (Needleman and Wunsch, 1970) the structurally conserved regions were built from the known structure of Mi_b-CK. Dimeric Mi_b-CK was used as a starting model. Two types of dimer can in principle be generated from the octamer by taking adjacent monomers in the octameric structure. Inspection of these two possible models, however, showed that only one satisfied several predictions for dimeric Mi_b-CK made from biochemical and biophysical experiments, such as the presence of certain tryptophan residues at the monomer-monomer interface (Gross and Wallimann, 1995). Subsequently, the structurally variable regions were built from corresponding locations in homologous proteins derived from a subset of the Brookhaven protein database. The resulting structure was then scanned for side-chain torsions to relieve bad van der Waals contacts and

energy minimized in several steps, employing the AMBER force field (Weiner et al., 1984, 1986) as implemented in the software package Sybyl 6.3. Initial validation of the model structure was done by checking for 1) the absence of hydrophobic residue exposure, 2) the presence of charged or polar side chains in the interior of the model, being inaccessible to solvent and not participating in salt bridges or hydrogen bonds, and 3) a positive free energy of solvation as recommended by Novotny et al. (1988).

RESULTS

Small-angle scattering in the presence of substrates

The desmeared scattering curves of Mi_b-CK and M-CK in the absence or presence of substrates are shown in Fig. 2. The scattering profile of Mi_b-CK closely resembled that of a more or less hollow sphere, whereas M-CK could be considered as a slightly elongated, ellipsoidal molecule. These data are consistent with the structural characterization by electron microscopy of Mi_b-CK octamers as cube-like particles with a central channel and of dimers as banana-shaped molecules (Schnyder et al., 1988). Upon binding of Mg-ATP or TSAC, considerable changes in the shape and the size of the molecules occurred, whereas creatine alone had only little effect. Fitting the linear parts of the scattering curves to straight lines in the Guinier representation allowed for the calculation of the smeared radii of gyration (R_g). For Mi_b-CK, the radius of gyration was reduced from 55.6 Å

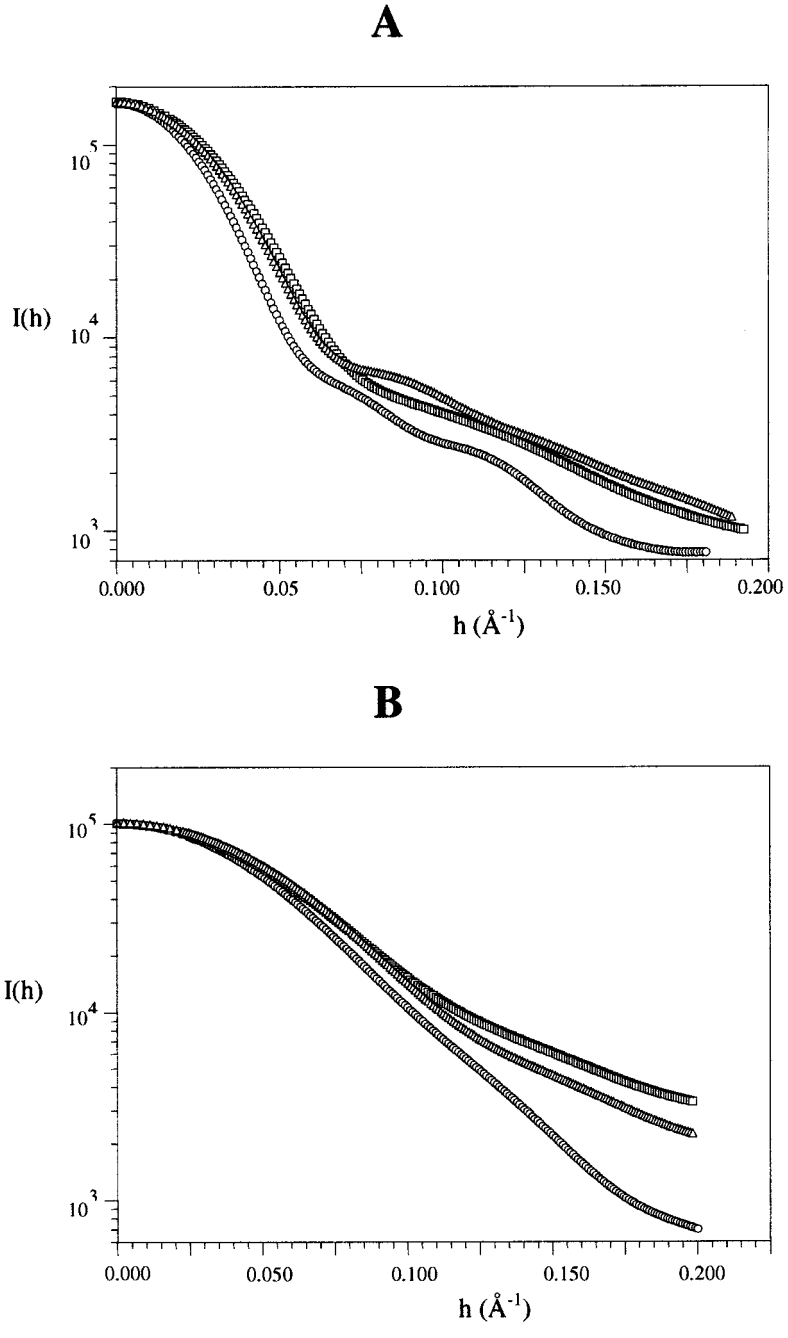

FIGURE 2 Small-angle x-ray scattering profiles of creatine kinase isoenzymes. Curves are shown as intensities of scattered radiation for free enzyme (○), enzyme plus Mg-ATP (□), and enzyme plus TSAC (△) as a function of the scattering vector h ($h = 4\pi \sin(\theta/\lambda)$ with 2θ being the scattering angle and λ being 1.5418 Å, the wavelength of the x-rays used). (*A*) Mitochondrial sarcomeric muscle isoform (Mi_b-CK); (*B*) cytosolic muscle-type isoform (M-CK).

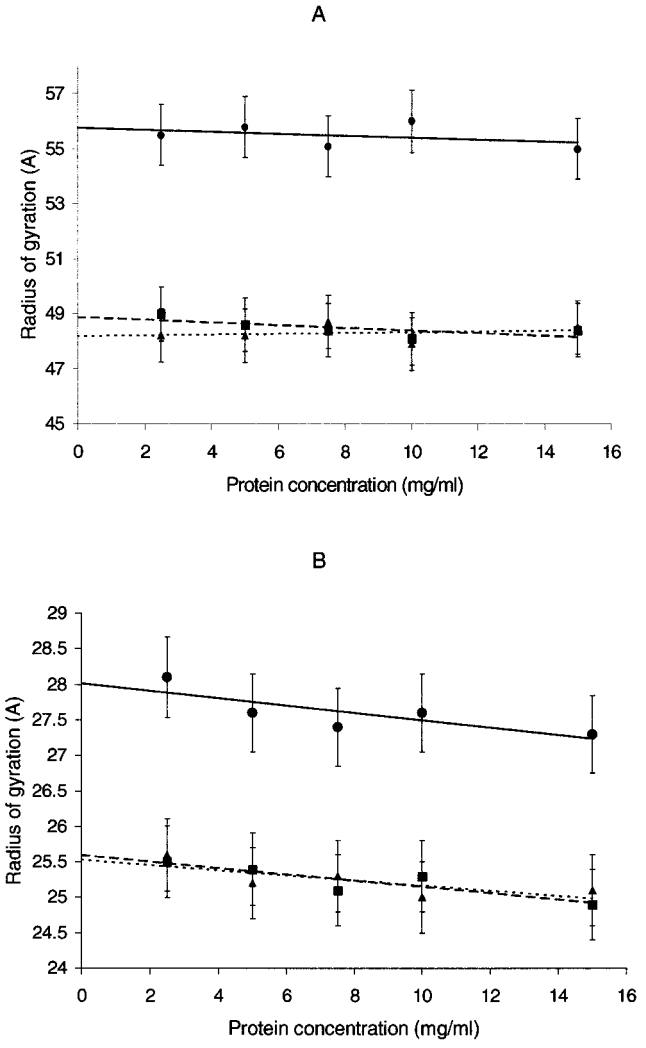

FIGURE 3 Concentration dependence of the radii of gyration. Radii of gyration derived from the Guinier representation of the scattering curves are plotted as function of creatine kinase concentration. ●, values for the free enzyme; ■, enzyme plus Mg-ATP; ▲, enzyme plus TSAC. (*A*) Mi_b-CK; (*B*) M-CK.

(free enzyme) to 48.9 Å (enzyme plus Mg-ATP) and to 48.2 Å (enzyme plus TSAC). The experiments performed with M-CK showed similar changes from 28.0 Å (free enzyme) to 25.6 Å (enzyme plus Mg-ATP) and to 25.5 Å (enzyme plus TSAC).

The distance distribution curves for M- and Mi_b-CK upon ligand binding are shown in Fig. 4. These curves were obtained by using a Fourier inversion of scattered intensity to derive a radial Patterson (P(*r*)) curve. The information in this curve is the length distribution of atom-weighted interatomic vectors in the particle. The P(*r*) curve of free Mi_b-CK shows the features of a roughly spherical particle, having a longest chord of approximately 160 Å. A significant decrease in the maximal chord length can be observed upon binding of TSAC or Mg-ATP. For M-CK, the P(*r*) curves cannot be interpreted as easily; however, the shape of the particle seems to be more elongated. Upon ligand binding, however, a more compact, spherical shape is obtained, as indicated by the shape of the P(*r*) curves. In the course of the calculation of the P(*r*) curves the desmeared R_g values were also derived. All relevant values of the smeared and desmeared R_g are found in Table 1. Creatine alone did not lead to significant changes in the radii of gyration, nor did free ATP or ADP, although x-ray crystallography revealed that ATP or a nonhydrolyzable analog (AMP-PNP) binds to the enzyme even in the absence of Mg^{2+} (Fritz-Wolf et al., 1996). SANS experiments performed with Mi_b-CK basically yielded the same results in the range of experimental error (data not shown). AK showed the same behavior: a change of the radius of gyration from 21.5 Å (free enzyme) to 19.7 Å (enzyme plus Mg-ATP), whereas with arginine alone only a minor change could be observed (see also Dumas and Janin, 1983).

All SAXS measurements were performed at two different temperatures, either at 4°C or 20°C. No significant differences in the scattering behavior of respective samples were observed at the two temperatures.

To control our samples for the existence of protein aggregates, we determined the radii of gyration at different protein concentrations and extrapolated to zero concentration. The relation of the determined values to protein concentration is shown in Fig. 3. There is no dependence of R_g on protein concentration found in our experiment. We therefore conclude that under the conditions used, no protein aggregation occurred either as a function of protein concentration or upon ligand binding. Furthermore, dissociation of the octamer as an explanation for the observed structural changes can be ruled out by this result.

We further determined the relative molecular masses (M_r) of the proteins from the scattering profiles. M_r is related to the normalized intensity extrapolated to zero-angle $I_n(0)$ (Luzatti, 1960). The values obtained from the values of $I_n(0)$ for the molecular masses, 340 ± 10 kDa for Mi-CK and 85 ± 6 kDa for M-CK, did not differ significantly from the values calculated from the amino acid composition of the proteins.

Additional control experiments with free phosphocreatine, Mg^{2+}, Mg^{2+} plus creatine or phosphocreatine, or creatine plus ADP in the absence of Mg^{2+} were performed. The data derived showed no significant differences to the data obtained from free enzyme or enzyme in the presence of free nucleotide or creatine (see Table 1).

Calculation of theoretical scattering profiles and model building

We calculated the scattering profile of Mi_b-CK in the presence of ATP from the x-ray crystallographic coordinates (Fritz-Wolf et al., 1996) and compared it with the experimentally obtained scattering curves. Fig. 5 shows the comparison of the experimentally obtained profiles and of the calculated one. The calculated profile resembles that of free Mi_b-CK, although there is no perfect fit, and differs signif-

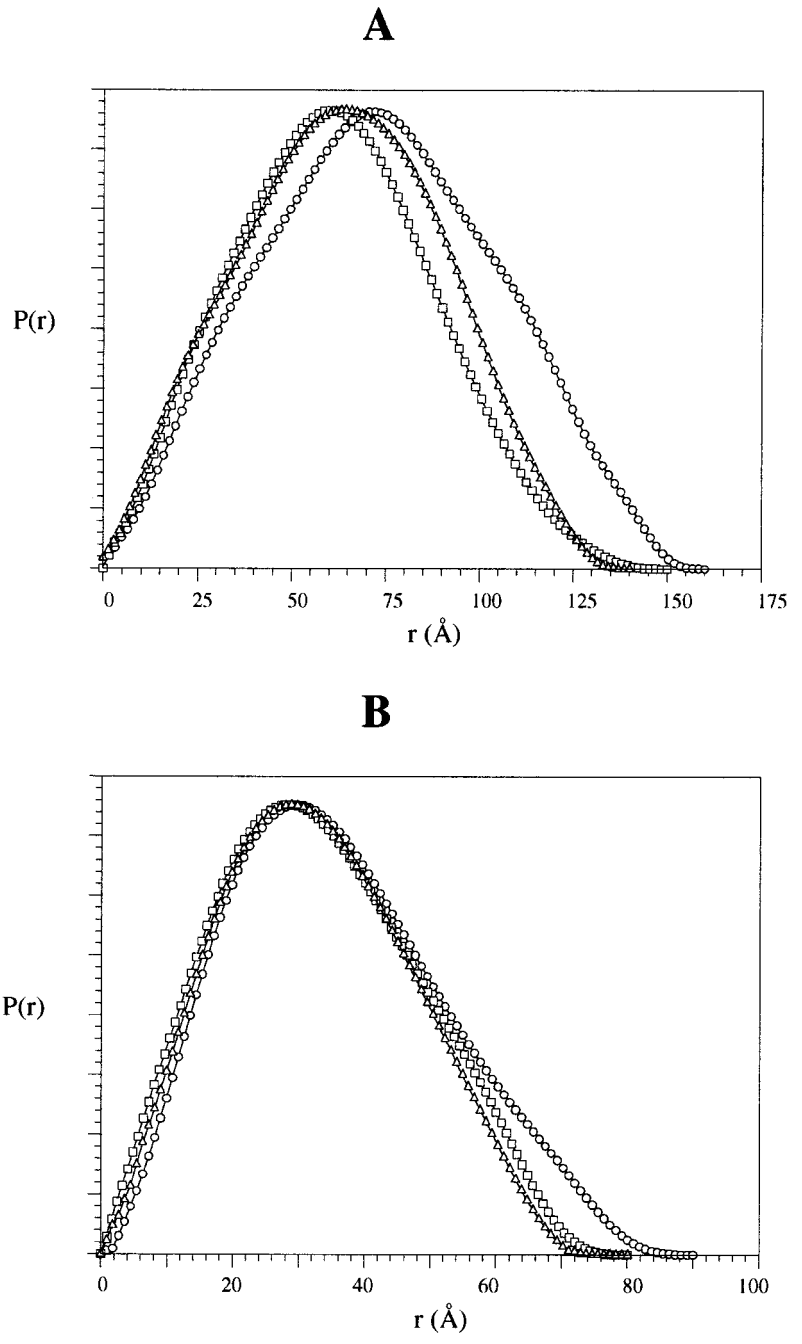

FIGURE 4 Radial distance distribution function P(*r*) from solution x-ray scattering data for creatine kinase. P(*r*) curves were calculated using the program ITP (Glatter, 1977) from data extrapolated to infinite dilution. Curves are shown for free enzyme (○), enzyme plus Mg-ATP (□), and enzyme plus TSAC (△). (*A*) Mi_b-CK; (*B*) cytosolic M-CK.

TABLE 1 Summary of parameters from SAXS experiments

	Smeared R_g (Guinier) (Å)	Desmeared R_g (Å)	d_{max}* (Å)
Mi-CK	55.6 ± 0.9	56.3	160
Mi-CK + Mg-ATP	48.9 ± 0.5	48.0	150
Mi-CK + TSAC	48.2 ± 0.5	46.9	145
Mi-CK + ATP	56.1 ± 0.8	56.3	160
Mi-CK + creatine	55.1 ± 1.1	55.8	160
M-CK	28.0 ± 0.4	28.0	89
M-CK + Mg-ATP	25.6 ± 0.4	25.5	81
M-CK + TSAC	25.5 ± 0.6	25.4	80
M-CK + ATP	28.0 ± 0.9	28.1	90
M-CK + creatine	28.3 ± 0.6	28.1	90

*d_{max}, longest chord in the molecule.

icantly from that of Mi_b-CK plus Mg-ATP. To investigate the spatial structure of dimeric cytosolic muscle-type M-CK for which hitherto no x-ray coordinates are available, we modeled the structure of a dimeric M-CK molecule from the x-ray coordinates of Mi_b-CK (Fritz-Wolf et al., 1996) as described in Materials and Methods. For an initial validation of the model we checked the absence of the parameters suggested by Novotny et al. (1988) for assessing the quality of a homology-built protein structure (see Materials and Methods). In addition, we compared the secondary structure distribution with that predicted from circular dichroism spectroscopy (Gross, 1994) and found good agreement (data not shown). This model was subsequently used for the

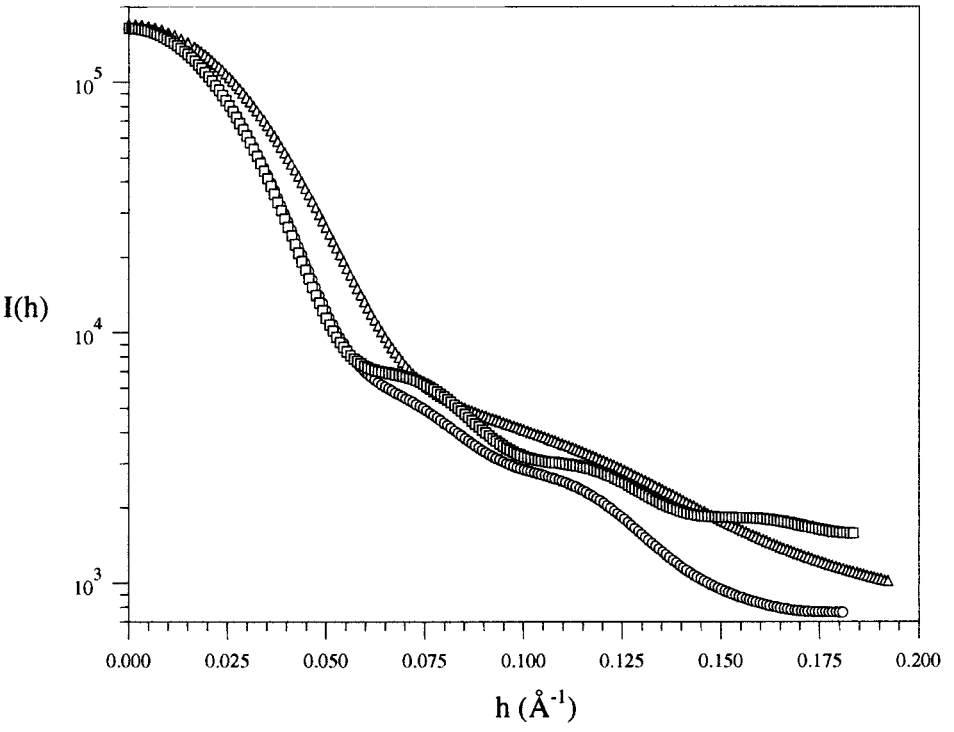

FIGURE 5 Comparison of scattering curves for Mi_b-CK. Curves are shown for the experimentally derived solution scattering curve (○) and for the scattering profile obtained by the method of Lattman (1989) from the crystallographic coordinates of octameric Mi_b-CK (□). The scattering profile of Mi-CK plus Mg-ATP is also included (△).

calculation of a theoretical small-angle scattering curve. The theoretical R_g of M-CK from the modeled structure is 26.9 Å compared with 28.0 Å for the experimentally derived value. The longest chord is 81 Å (82 Å in the experimental curve), the P(*r*) curves show some, albeit small, differences in shape (Fig. 6).

DISCUSSION

Our small-angle scattering measurements indicate that creatine kinase isoenzymes undergo major conformational changes upon ligand binding, large enough to affect both radii of gyration and maximal diameter of the proteins. Interestingly, binding of ATP or ADP in the absence of Mg^{2+} did not lead to a significant change in the size or shape of either of the enzymes examined. We know, however, from x-ray crystallography that free ATP or nonhydrolyzable analogs thereof (e.g., AMP-PNP) can bind to Mi_b-CK (Fritz-Wolf et al., 1996), although the position of the bound Mg^{2+}-free nucleotide is most likely not the same as that expected for the Mg-nucleotide. Therefore, we calculated the scattering profile of Mi-CK in the presence of

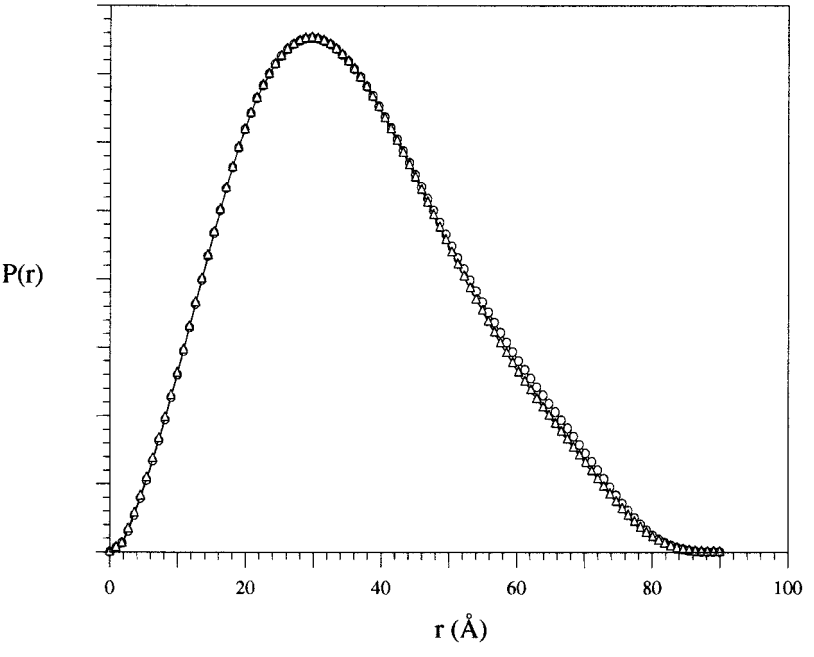

FIGURE 6 Comparison of the distance distribution functions for cytosolic M-CK. Curves are shown for the experimentally obtained scattering profile (○) and for the *P*(*r*) function calculated from the model coordinates of M-CK (△).

bound ATP from the coordinates obtained by x-ray crystallography and compared it with the experimentally derived scattering curves. From this experiment one can conclude that the three-dimensional structure of Mi_b-CK in the presence of ATP resembles the structure of free Mi_b-CK in solution, which is significantly different from that of Mi_b-CK in the presence of either Mg-ATP or TSAC. The small differences in shape between the calculated scattering curve and the experimentally obtained scattering curve of free Mi_b-CK can be attributed to highly ordered water molecules in the central channel of the octameric Mi_b-CK complex. Such water molecules in central cavities or channels, which have recently been shown by infrared spectroscopy to be present in the central channel of Mi_b-CK (U. Fringeli, personal communication), cannot be properly included in the theoretical calculation of the small-angle scattering curve by the algorithm used, and hitherto no way around this problem has been found, either by us or by others.

Furthermore, it is obvious that neither ATP nor ADP alone nor free Mg^{2+} can induce a significant conformational change in Mi_b-CK, but that the Mg-nucleotide is needed for this transition to occur. This is of great importance for the interpretation of the three-dimensional structure of Mi-CK, especially in terms of the elucidation of the catalytic pathway. We propose to call the conformations of free M- and Mi_b-CK open conformations, whereas those in the presence of Mg-ATP or TSAC should be considered as closed conformations. The small differences between the Mg-ATP- and TSAC-bound enzymes observed in our experiments cannot be considered significant, and one can assume that the obvious differences in the molecular structures of these two states are of a magnitude that is not experimentally accessible by SAXS.

Monomeric arginine kinase also showed a decrease in R_g of 1.2 Å upon binding of Mg-ATP, which is consistent with previous results obtained with this enzyme (Dumas and Janin, 1983). Similar experiments have been performed with other enzymes from different protein families; e.g., both yeast hexokinase (McDonald et al., 1979) and yeast phosphoglycerate kinase (Pickover et al., 1979) exhibit a decrease of their radii of gyration of similar magnitude. From crystallographic studies of hexokinase, crystallized in the presence or absence of glucose, the nature of this conformational change is known (Bennet and Steitz, 1980a,b). A domain movement of one of the two domains in hexokinase by a rotation of 10° relative to the other, resulting in a movement of up to 9 Å in combination with a closure of the cleft where glucose is bound, is responsible for the conformational change. Calculations of the solution scattering profiles of the different protein conformations and comparison with the experimental data showed that the changes in R_g are the same, confirming the existence of the domain movements in solution (McDonald et al., 1979). Dumas and Janin (1983) concluded from their data that a similar movement might cause the conformational change in arginine kinase, although Mg-nucleotide rather than arginine binding induced the domain movement. So far, we have not been able to obtain crystallographic data of Mi-CK in the presence of Mg-ATP or TSAC. Therefore, we tried to calculate scattering profiles for a closed conformation of Mi-CK by simulating a rotation of the domains relative to each other in the same order of magnitude as seen with hexokinase and as suggested for AK (indicated by bent arrows in Fig. 1). Although a decrease in the calculated R_g values was obtained, it was not as large as seen experimentally (M. Forstner, unpublished observations). Even if further movements of the C1 and C2 subdomains are considered, this does not lead to the pronounced changes observed. We therefore conclude that another additional type of movement must be involved in the large conformational change observed for Mi-CK. This might be a movement of the dimeric building blocks of the octamer relative to each other, thereby also inducing the change in globularity observed upon ligand binding. Such a movement could be envisaged because dimer-dimer contacts in the Mi_b-CK octamer are rather weak and because the long axes of the dimers are slightly skewed relative to the fourfold axis of the octamer, making a spring-like movement of the latter possible.

The slightly smaller values of R_g for the enzymes in presence of TSAC compared with the radii observed in the presence of Mg-nucleotide are most probably without any relevance, as the error of the experimental method is larger than the observed differences.

Despite numerous attempts by different groups to crystallize and solve the high-resolution structure of M-CK, no x-ray structure of this isoenzyme could hitherto be derived. We have therefore modeled the structure of chicken M-CK from the x-ray structure coordinates of chicken Mi_b-CK by homology modeling and compared the experimentally observed scattering curves and derived distance distribution functions with those calculated from the model coordinates. As the degree of primary structure identity between these two isoenzymes is nearly 75% (Mühlebach et al., 1994), we assume that such an approach is valid. As can be seen from Fig. 6, the observed and calculated distance distribution curves agree quite well with each other, although there are some differences that, however, might yield from ordered water molecules in the first solvation shell of the enzyme that could not be properly included in the theoretical calculations. Together with the good agreement of the model secondary structure prediction with the circular dichroism spectroscopic data (Gross, 1994) the results of the small-angle scattering study suggest that the model derived from a mitochondrial Mi_b-CK dimer is, indeed, a valid model for the structure of cytosolic M-CK. This model structure might also be better suited for the application of molecular replacement techniques to solve the x-ray structure of M-CK.

Furthermore, an important consideration regarding the evolutionary position of guanidino kinases arises from our observation. In the case of other phosphagen kinases (e.g., hexokinase or phosphoglycerate kinase), it is the actual substrate (i.e., glucose or phosphoglycerate) that causes a

structural change upon binding, whereas binding of the Mg-nucleotide leaves the overall structure of these enzymes unperturbed. This, together with the significant difference in the fold of guanidino kinases and other kinases gives strong support to the assumption that guanidino kinases may have evolved on a different pathway than other phosphagen kinases. It remains to be seen whether a detailed analysis of the enzymatic mechanism from emerging high-resolution structures of CK in the presence of substrates will unveil a hitherto unknown mechanism for the kinase reaction.

We hope that with the emergence of a high-resolution three-dimensional structure of Mi-CK in the presence of substrates, we might also be able to fully interpret the experimentally obtained small-angle scattering curves and that the long-awaited solution of the structure of cytosolic M-CK will allow for a comparison of the modeled and experimentally derived structures.

We thank Prof. H. Stuhrmann for giving us access to his neutron beamline at the GKSS, Geesthacht, Germany, and Dr. R. Willumeit for experimental help there, Dr. D. Rognan and Prof. G. Folkers (ETH Zürich, Department of Pharmacy) for help with molecular modeling software, Dr. M. Stolz for providing recombinant M-CK, and the CK group at the ETH Zürich for discussions. We also thank Prof. E. E. Lattman, Johns Hopkins University, Baltimore, MD, for providing FORTRAN code and Mr. K. Nedwed, Bio-Rad/Softshell, Grand Junction, CO, for helpful hints on C++ programming.

This work was supported by an ETH grant to T. Wallimann and M. Forstner and a grant of the Swiss National Science Foundation (31–33907.92) to T. Wallimann.

REFERENCES

Bennet, W. S., and T. A. Steitz. 1980a. Structure of a complex between yeast hexokinase A and glucose. I. Structure determination and refinement at 3.5 Å resolution. *J. Mol. Biol.* 140:183–209.

Bennet, W. S., and T. A. Steitz. 1980b. Structure of a complex between yeast hexokinase A and glucose. II. Detailed comparisons of conformation and active site configuration with the native hexokinase B monomer and dimer. *J. Mol. Biol.* 140:211–230.

Bradford, M. M. 1976. A rapid and sensitive method for the quantitation of microgram quantities of protein utilizing the principle of protein-dye binding. *Anal. Biochem.* 72:248–254.

Brünger, A. T. 1991. Simulated annealing in crystallography. *Annu. Rev. Phys. Chem.* 42:197–223.

Dumas, C., and J. Janin. 1983. Conformational changes in arginine kinase upon ligand binding seen by small-angle x-ray scattering. *FEBS Lett.* 153:128–130.

Forstner, M., M. Kriechbaum, P. Laggner, and T. Wallimann. 1996. Changes of creatine kinase structure upon ligand binding as seen by small-angle scattering. *J. Mol. Struct.* 383:217–222.

Fritz-Wolf, K., T. Schnyder, T. Wallimann, and W. Kabsch. 1996. Structure of mitochondrial creatine kinase. *Nature*. 381:341–345.

Furter, R., P. Kaldis, E. M. Furter-Graves, T. Schnyder, H. M. Eppenberger, and T. Wallimann. 1992. Expression of active octameric chicken cardiac mitochondrial creatine kinase in *Escherichia coli*. *Biochem. J.* 288:771–775.

Glatter, O. 1977. A new method for the evaluation of small-angle scattering data. *J. Appl. Crystallogr.* 10:415–421.

Gross, M. 1994. The tryptophan residues of mitochondrial creatine kinase: roles in enzyme structure and function. Ph.D. thesis (ETH 10719). Swiss Federal Institute of Technology, Zürich, Switzerland.

Gross, M., and T. Wallimann. 1993. Kinetics of assembly and dissociation of the mitochondrial creatine kinase octamer: a fluorescence study. *Biochemistry*. 32:13933–13940.

Gross, M., and Wallimann, T. 1995. Dimer-dimer interactions in octameric mitochondrial creatine kinase. *Biochemistry*. 34:6660–6667.

Kirkpatrick, S., C. D. Gelatt, Jr., and M. P. Vecchi. 1983. Optimization by simulated annealing. *Science*. 220:671–680.

Kraulis, P. J. 1991. MOLSCRIPT: a program to produce both detailed and schematic plots of protein structures. *J. Appl. Crystallogr.* 24:946–950.

Laggner, P., and H. Mio. 1992. SWAX: a dual-detector camera for simultaneous small- and wide-angle x-ray diffraction in polymer and liquid crystal research. *Nucl. Instrum. Methods Phys. Res. A*. 323:86–90.

Lattman, E. E. 1989. Rapid calculation of the solution scattering profile from a macromolecule of known structure. *Proteins Struct. Funct. Genet.* 5:149–155.

Luzatti, V. 1960. Interpretation des mesures absolues de diffusion centrale des rayons X en collimation ponctuelle ou lineaire: solutions de particules globulaires et de Bâtonnets. *Acta Crystallogr.* 13:939–945.

McDonald, R. C., T. A. Steitz, and D. M. Engelman. 1979. Yeast hexokinase in solution exhibits a large conformational change upon binding glucose or glucose-6-phosphate. *Biochemistry*. 18:338–342.

Milner-White, E. J., and Watts, D. C. 1971. Inhibition of adenosine 5′-triphosphate-creatine phosphotransferase by substrate-anion complexes. *Biochem. J.* 122:727–740.

Mühlebach, S., M. Gross, T. Wirz, T. Wallimann, J. C. Perriard, and M. Wyss. 1994. Sequence homology and structure predictions of the creatine kinase isoenzymes. *Mol. Cell. Biochem.* 133/134:245–263.

Needleman, S., and C. Wunsch. 1970. A general method applicable to the search for similarities in the amino acid sequence of two proteins. *J. Mol. Biol.* 48:443–453.

Novotny, J., A. A. Rashin, and R. E. Bruccoleri. 1988. Criteria that discriminate between native proteins and incorrectly folded models. *Proteins Struct. Funct. Genet.* 4:19–30.

Pickover, C. A., D. B. McCay, D. M. Engelman, and T. A. Steitz. 1979. Substrate binding closes the cleft between the domains of yeast phosphoglycerate kinase. *J. Biol. Chem.* 254:11323–11329.

Rojo, M., R. Hovius, R. Demel, K. Nicolay, and T. Wallimann. 1991. Mitochondrial creatine kinase mediates contact formation between mitochondrial membranes. *J. Biol. Chem.* 266:20290–20295.

Schnyder, T., A. Engel., A. Lustig, and T. Wallimann. 1988. Native mitochondrial creatine kinase forms octameric structures. II. Characterization of dimers and octamers by ultracentrifugation, direct mass measurements by scanning transmission electron microscopy, and image analysis of single mitochondrial creatine kinase octamers. *J. Biol. Chem.* 263:16954–16962.

Schnyder, T., D. F. Sargent, T. J. Richmond, H. M. Eppenberger, and T. Wallimann. 1990. Crystallization and preliminary x-ray analysis of two different forms of mitochondrial creatine kinase from chicken cardiac muscle. *J. Mol. Biol.* 216:809–812.

Wallimann, T., T. Schlösser, and H. M. Eppenberger. 1984. Function of M-line bound creatine kinase as intramyofibrillar ATP regenerator at the receiving end of the phosphocreatine shuttle. *J. Biol. Chem.* 259: 5238–5246.

Wallimann, T., M. Wyss, D. Brdiczka, K. Nicolay, and H. M. Eppenberger. 1992. Intracellular compartmentation, structure and function of creatine kinase isoenzymes in tissues with high and fluctuating energy demands: the 'phosphocreatine circuit' for cellular energy homeostasis. *Biochem. J.* 281:21–40.

Weiner, S. J., P. Kollman, D. A. Case, U. C. Singh, G. Ghio, G. Alagona, S. Profeta, and P. K. Weiner. 1984. A new force field for molecular mechanics simulation of nucleic acids and proteins. *J. Am. Chem. Soc.* 106:765–784.

Weiner, S. J., P. Kollman, D. T. Nguyen, and D. A. Case. 1986. An all atom force field for simulations of proteins and nucleic acids. *J. Comput. Chem.* 7:230–252.

Wyss, M., J. Smeitink, R. A. Wevers, and T. Wallimann. 1992. Mitochondrial creatine kinase: a key enzyme of aerobic energy metabolism. *Biochim. Biophys. Acta* 1102:119–166.